www.amlett.com, www.amlett.org, DOI: 10.5185/amlett.2012.11466 Published online by the VBRI press in 2013

Post-deposition annealing controlled structural and optical properties of RF magnetron sputtered MoO_3 films

S. Subbarayudu*, V. Madhavi, S. Uthanna

Department of Physics, Sri Venkateswara University, Tirupati 517502, India

*Corresponding author. Tel: (+91) 9849700207; E-mail: srsuguru.phy@gmail.com

Received: 17 November 2012, Revised: 06 January 2013 and Accepted: 12 January 2013

ABSTRACT

MoO_3 films were deposited on Corning glass and silicon substrates held at room temperature (303 K) by RF magnetron sputtering of metallic molybdenum target at a fixed oxygen partial pressure of $4x10^{-4}$ mbar and sputter pressure of $4x10^{-2}$ mbar. The as deposited films were annealed in air at different temperatures in the range 473 – 673 K. X-ray diffraction studies suggest that the as-deposited and the films annealed at 473 K were amorphous in nature, while those annealed at 573 and 673 K were polycrystalline with mixed phases of α- orthorhombic and β- monoclinic MoO_3. Scanning electron microscope images of the films annealed at 573 and 673 K exhibited nanoflower like and nanodisk like structures due to improvement in the crystallinity. Fourier transform infrared studies showed the characteristic vibrations of MoO3 with shift in the vibrational modes of Mo = O and Mo – O – Mo with increase of annealing temperature. The optical absorption edge of the films shifted towards lower wavelengths side with increase of annealing temperature. Optical band gap of as-deposited films was 2.98 eV with refractive index 2.01, while those annealed at 673 K showed the optical band gap of 3.15 eV and refractive index of 2.08. The MoO_3 films annealed at 673 K were of nanocrystalline with crystallite size of 39 nm with optical band gap of 3.15 eV and refractive index of 2.08 were favorable for electron blocking and hole-selective layers in bulk-heterojuction solar cells.
Copyright © 2013 VBRI press.

Keywords: RF sputtering; molybdenum oxide; post-annealing; structural; optical properties.

S. Subbarayudu is presently research scholar under the guidance of Prof. S. Uthana, Dept. Physics, Sri Venkateswara University, Tirupathi, India. Currently he is working on the RF magnetron sputtered MoO_3 films. He received his Master Degree in Physics from the Sri Krishnadevaraya University, Anantapur, India during the year 1993-95.

Introduction

Molybdenum oxide (MoO_3) is a material finds potential applications due to its abundance and attractive properties such as catalyst, gas sensing and electrochromism **[1-4]**. MoO_3 thin films exist in three phases namely: orthorhombic α- phase, monoclinic β- phase and hexagonal phase. The crystal structure of β- MoO_3 in which MoO^{6+} octahedral form a three dimensional network by sharing the corners with each other and well suited as a catalyst for number of chemical reactions. The amorphous MoO_3 films formed by sol-gel dip coating exhibited electrochromic properties **[5].** The lithium ions inserted into α- MoO_3 films lead to an increase in the charge storage capacity **[6]**. Orthorhombic α- MoO_3 nanoflakes were find applications in the cold cathode based electronics **[7]**. Recently, nanocrystalline oxide films attracted much for their promising applications in building of nanodevices and nanosensors **[8-11].** Kocak et al. **[12]** realized the catalytic activity of electrodeposited MoO_3 for nitrite oxidation. Allogho and Ashrit **[13]** reported on the photochromic activity of MoO_3 films prepared by thermal evaporation to gauge the water content. Molybdenum oxide is a promising candidate for a back contact layer for cadmium telluride solar cells in superstrate configuration because of its high work function, possibly reducing the back contact barrier **[14].** Various thin film deposition techniques such as thermal evaporation **[15],** pulsed laser deposition **[16, 17]**, sputtering **[5, 18-20],** atomic layer deposition **[21]**, electrodeposition **[22, 23],** spray pyrolysis **[2],** sol – gel process **[6, 24, 25]** and hot wire chemical vapour deposition **[26]** were employed for growth of MoO_3 films. The phase, structure and surface morphology of the deposited films depend critically on the growth parameters and the adopted thin films deposition technique. The post-deposition annealing in air at different

 Copyright © 2013 VBRI press.

temperatures leads to the structural modification of the films **[3, 5, 9]**. Chang et al. **[3]** reported on the effect of air annealing at temperatures in the range 493 - 823 K in RF magnetron sputtered MoO_3 films. The films annealed between 623 - 673 K were composed mixed phase of α- and β- phase MoO_3, while < 623 K were single phase of β - MoO_3 which is potential for ammonia sensing. Dhanasankar et al. **[5]** reported on the sol-gel coated MoO_3 films that the optical band gap increased from 3.53 to 3.73 eV with increase of annealing in air at temperatures from 473 to 523 K and at higher temperatures of 723 K it decreased to 3.63 eV. Lin et al. **[9]** reported on the electron beam evaporated MoO_3 films, and subsequently annealed in N_2 and O_2 for 10 min by rapid thermal annealing. The predominant β- MoO_3 was achieved at annealing temperatures < 573 K, where as α - MoO_3 realized at 673 K. The optical band gap of the films decreased from 3.93 to 3.89 eV with increase of annealing in N_2 from 473 to 773 K. The films annealed in O_2 the band gap increased from 3.93 to 3.97 eV with increase of annealing temperatures from 473 to 773 K. From these studies, it revealed that the crystallographic structure and optical band gap of the MoO_3 films critically depend on the annealing temperatures and ambient of annealing. Uthanna et al [**19**] reported on the DC magnetron sputtered MoO_3 films formed at room temperature were of amorphous while those deposited at 473 K were orthorhombic phase. The optical band gap increased from 3.03 to 3.28 eV and the refractive index increased from 2.03 to 2.08 with increasing substrate temperatures from 303 to 473 K due to improvement in the crystallinity of the films. In the present investigation, an attempt is made in the deposition of MoO_3 films at room temperature by RF magnetron sputtering and studied the effect of post-deposition annealing in air on the structural and morphological and optical properties.

Experimental

Preparation of MoO_3 thin films

MoO_3 thin films were deposited onto glass and silicon substrates held at room temperature (303 K) by sputtering of pure metallic molybdenum target in oxygen and argon gas mixture using reactive RF magnetron sputtering technique. Metallic molybdenum target (99.99 % pure) with 50 mm diameter and 3 mm thickness was used for sputtering. The sputter chamber was evacuated by employing diffusion pump and rotary pump combination to achieve base pressure of 4×10^{-6} Pa. Pressure in the sputter chamber was measured with digital Pirani – Penning gauge combinations. Oxygen and argon of 99.99 % purity were used as reactive and sputter gases for deposition of films. After achieving ultimate pressure, oxygen gas was introduced to the sputter chamber to a pressure of 4×10^{-4} mbar. Later, argon gas was admitted to the sputter pressure of 4×10^{-2} mbar. The required quantities of oxygen and argon gases were admitted into the sputter chamber through fine controlled needle valves followed by Aaloburg mass flow controllers (Model GFC 17). The 150 W power was supplied to the sputter target using RF power generator (Advance Energy Model ATX-600W). The sputter parameters fixed during the growth of the films are given in **Table 1.** The as-deposited films were annealed in air for 2 hours at different temperatures in the range 473 – 673 K.

Characterization

The as-deposited and the MoO_3 films annealed at different temperatures were characterized by studying their chemical composition, crystallographic structure and surface morphology, chemical binding configuration and optical properties. The thickness of the deposited films was measured with a mechanical Veeco Dektak (Model 150) depth profilometer. A force of 10 μN was applied over the sample surface with a swept length of 3 mm for 100 sec. The chemical composition of the films was analysed with energy dispersive X-ray Analysis (Oxford instruments Inca Penta FETx3) attached to a scanning electron microscope (Carl Zeiss, model EVO MA15). The crystallographic structure of the films was determined by using X-ray diffractometer (Bruker D8 Advance Diffractometer) with copper K_α radiation wavelength of $\lambda = 0.15406$ nm. The XRD profiles were taken for a 2θ range between 10^0 and 60^0 at the steps of 0.05°. The surface morphology of the films was analysed with scanning electron microscope (Hitachi SEM Model S-400). The chemical binding configuration of the films formed on silicon substrates was analyzed with Fourier transform infrared spectrophotometer (Nicolet Magana IR 750) was used to record the transmittance in the wavenumber range 300 – 1500 cm^{-1}. The optical transmittance of the films formed on glass substrates was recorded using UV-Vis-NIR double beam spectrophotometer (Perkin - Elmer Spectrophotometer Lamda 950) in the wavelength range 300 - 1500 nm.

Table 1. Sputter parameters fixed during the growth of the MoO_3 films.

Parameter	Value
Sputter target	: Molybdenum (50 mm × 3 mm)
Target to substrate distance	: 65 mm
Ultimate pressure	: 4×10^{-6} mbar
Oxygen partial pressure (pO_2)	: 4×10^{-4} mbar
Sputtering pressure	: 4×10^{-2} mbar
Sputter power	: 150 W
Deposition time	: 120 min

Results and discussion

Composition analysis

The thickness of the deposited films was determined by using Veeco Dektak depth profilometer was in the range 910 - 980 nm. The chemical composition of the MoO_3 films was determined by using energy dispersive X-ray analysis (EDAX). **Fig. 1** shows the EDAX spectrum of the as-deposited MoO_3 film. The spectrum contained characteristic constituents of molybdenum and oxygen in

Copyright © 2013 VBRI press

the film. The chemical composition of the films was determined from the peaks of molybdenum and oxygen. The atomic ratio of oxygen to molybdenum was 2.98: 1. It indicated that the as-deposited films were nearly stoichiometric. It remains almost constant in the films annealed in air at different temperature.

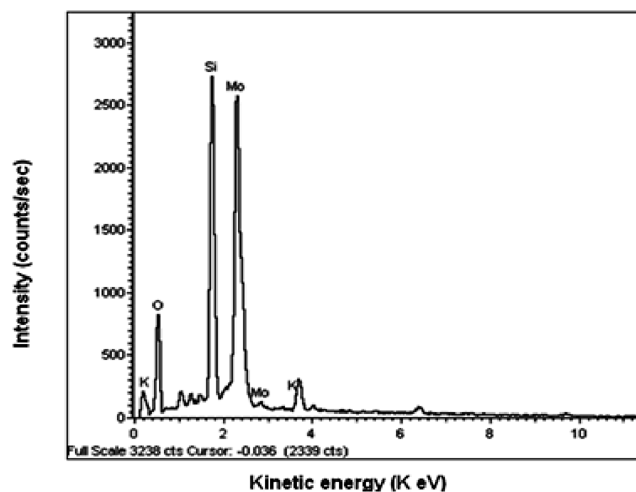

Fig. 1. EDAX spectrum of as deposited MoO_3 film.

XRD study

Fig. 2 shows the XRD profiles of as-deposited and the MoO_3 films annealed at different temperatures. The as-deposited MoO_3 films showed no characteristic diffraction peaks which indicated that the grown films were amorphous in nature. The mobility of ad-atoms arriving on the substrate surface will be low in the as-deposited films and the interaction between the molybdenum and oxygen will be low hence of amorphous nature. The films annealed in air at 473 K were also amorphous (not shown in **Fig. 2**). It indicated that the thermal energy gained by annealing at 473 K was not sufficient to initiate crystallization of the amorphous phase MoO_3 films. Post-deposition annealing of the films at 573 K exhibited the orientations (020), (040) and (060) related to the growth of orthorhombic α- phase MoO_3 [JCPDS card No. 76 - 1003]. The additional reflections of (011) and (201) were also present, which related to the growth of monoclinic β- phase [JCPDS card No 86 – 1269]. It revealed that the films annealed at 573 K were of mixed phase of orthorhombic α-phase and monoclinic β- phase MoO_3. Further increase of annealing temperature to 673 K, three additional (102), (110) and (400) reflections were also observed due to the formation of β- phase MoO_3 associated with α- phase MoO_3.Thus, the as-deposited and the films annealed at 473 K were amorphous and the crystallinity of films increased with the increase of annealing temperatures ≥ 573 K and associated with the mixed phase of α- phase and β- phase MoO_3. The results achieved are in accordance with the reports of Chang et al. **[3]** where α- and β- phase films were achieved by annealing of RF magnetron sputtered MoO_3 films in the temperatures in the range 623 - 673 K, and single phase α-MoO_3 films at 723 K. Navas et al. **[21]** achieved monoclinic Mo_8O_{23} and orthorhombic MoO_3 phases by annealing of RF magnetron sputtered molybdenum oxide films annealed at 573 and 673 K respectively.

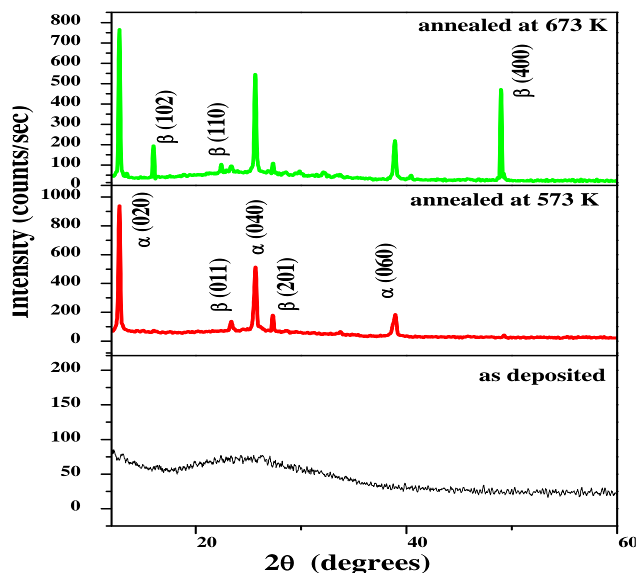

Fig. 2. XRD profiles of as-deposited and annealed MoO_3 film.

Mahammad et al. **[27]** achieved amorphous films on unheated substrates by DC magnetron sputtering. The films formed at high oxygen partial pressure of 0.4 Pa and annealed at 823 K were completely transformed in to α-phase MoO_3 where as those formed at low oxygen partial pressure of 0.19 Pa showed weaker α- MoO3 peaks with a weak β- MoO3 contribution after annealed at 873 K. Fan et al. **[28]** reported that films deposited at substrate temperatures of 573 and 673 K by RF magnetron sputtering exhibited the growth of β- phase Mo_9O_{26} and α-phase MoO_3. Yang et al. **[29]** reported that β- phase MoO_3 films at substrate temperature of 473 K and α- phase at temperatures ≥ 573 K in electron beam evaporated films. Thus, the crystillinity increased with increase of annealing temperature which leads to the growth of nanocrystalline structure of MoO_3. The crystallite size (L) of the films were calculated from the X-ray diffraction peaks by using Debye - Scherrer's relation **[30]**.

$$\text{Crystallite size, } L = 0.89\lambda / \beta \cos\theta \quad (1)$$

where λ is the wavelength of the X-ray (0.15406 nm), β the full width at half maximum of diffraction intensity measured in radians and θ the diffraction angle. The crystallite size of the films increased from 32 and 39 nm with increase of annealing temperature from 573 and 673 K respectively. Thus, crystallite size increased with increase of annealing temperatures as noticed by decreasing in the width of FWHM. This confirms that the amorphous MoO_3 films were modified into nanocrystalline with annealing temperature. The dislocation density (δ) and strain (ε) developed in the films were calculated from the crystallite size using the relations **[31],**

$$\text{Dislocation density, } \delta = 1/L^2 \quad (2)$$

$$\text{and, Strain, } \varepsilon = \beta \cos\theta/4 \quad (3)$$

 Copyright © 2013 VBRI press

The dislocation density of the films decreased from the 7.6 x 10^{14} to 6.3 x 10^{14} line/m^2 with increase of annealing temperature from 573 to 673 K respectively. The strain developed in the films also decreased from 9.5×10^{-4} to 8.7×10^{-4} line/m^2 with increase of annealing temperature from 573 to 673 K respectively as shown in **Table 2**. The thermal energy gained by annealing leads to rearrangement of atoms takes place and increase in the crystallite size. The increase of crystallite size leads to decrease in the grain boundary area which will decrease in the dislocation density. When the dislocation density decreased the strain in the films also decreased.

Table 2. FWHM, crystallite size, strain and dislocation density of MoO_3 films.

Temperature	FWHM (Degree)	Crystallite size (nm)	Strain (Line^{-2}m^{-1})	Dislocation density (Line/m^2)
As- deposited	---	---	---	---
Annealed at 573 K	0.218	32	9.5x10^{-4}	7.6x10^{14}
Annealed at 673 K	0.202	39	8.7x10^{-4}	6.3x10^{14}

Surface morphology

Fig. 3 shows the scanning electron micrograph images of the as-deposited and the MoO_3 films annealed at different temperatures. SEM of as-deposited films showed smooth surface morphology because of the amorphous phase. The films annealed at 573 K showed the nanoflowers like grain structure with the grain size of 3 µm. At higher annealing temperatures the molecules acquired the required thermal energy to promote the growth of films with larger size grains that is the growth of polycrystalline MoO_3 films with mixed phase. Yang et al. **[29]** reported on the formation of platelet nanocrystallites uniformly distributed over the surface. In the present work, the films annealed at 673 K were of nanodisk like structure with grain size of about 800 nm, due to the coalescence of neighboring crystallites driven by thermal energy by annealing. The change in surface morphology with different annealing temperatures was due to the modification of grain growth in to nanocrystalline with uniform size of crystallites. The morphological studies revealed that, the annealed films exhibited the layered structure at high annealing temperatures with enhancement in the crystallinity.

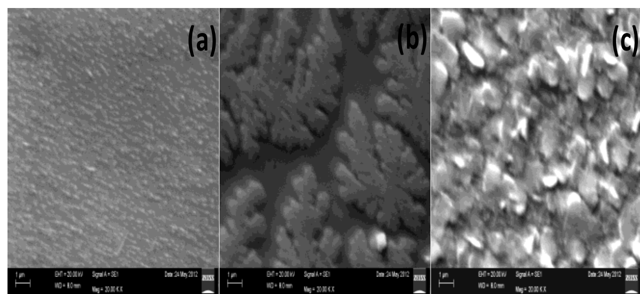

Fig. 3. SEM images of MoO_3 films formed at a) 303 K, and annealed at b) 573 K and c) 673 K.

Fourier transforms infrared spectroscopy

Fourier transform infrared transmittance spectra of as-deposited and annealed MoO_3 films formed on silicon substrates were recorded in the wavenumber range 300 – 1500 cm^{-1} **(Fig. 4)**. The FTIR spectra of as-deposited films contained broad band in between wavenumbers 600 and 1000 cm^{-1}. There were three weak absorption bands at 795, 668 and 570 cm^{-1} which related to two stretching vibrational modes of Mo= O, Mo - O and one transverse optical vibrations mode of Mo - O - Mo **[21]**. The FTIR spectra of the films annealed at 573 K showed the intense absorption bands at about 812, 672 and 573 cm^{-1}. The absorption band observed at 812 cm^{-1} was attributed to the binding vibrations of Mo = O in Mo^{6+} of the α– phase MoO_3 **[20]**. The films annealed at 673 K showed shift in the bands to 817, 681 and 563 cm^{-1}. The intensity of IR absorption bands was increased with increase of annealing temperature. This may be due to enhancement in the ad-atom mobility at high annealing temperatures, hence improved the crystallinity of the films. The intensity of the absorption band at 991 cm^{-1} was associated with the Mo = O stretching vibration and intensity enhanced with the increase of annealing temperature. Dhanasankar et al. **[5]** reported that weak absorption peak at 567 cm^{-1} which represents Mo - O - Mo band and the terminal Mo = O double bands characterized by absorption bands appearing around 885 - 1007 cm^{-1}. Ivanova et al. **[32]** also noticed, a strong band at 820 cm^{-1} and a weak absorption band at 545 cm^{-1}, which represent the stretching vibrational modes of Mo= O, and transverse optical vibrations mode of Mo-O-Mo for orthorhombic MoO_3 films annealed at 673 K.

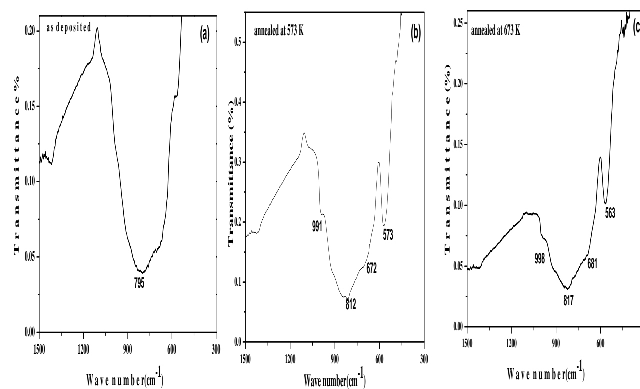

Fig. 4. FTIR spectra of MoO_3 films: (a) as-deposited, and annealed at: (b) 573 K and (c) 673 K.

Optical property

Fig. 5 shows the optical transmittance spectra of as-deposited and annealed MoO_3 films recorded in the wavelength range 300 - 1500 nm. The as-deposited films showed an average transmittance of 60 % (at wavelengths > 600 nm). The films annealed at higher temperatures showed about 85 % transmittance. The low transmittance in the as-deposited films was due to the presence of oxygen vacancies which can scatter the light photons hence the reduced transmittance. The increase of annealing temperature leads to reduction in the oxygen vacancies hence improved crystallinity, hence improved the transmittance. The optical absorption edge of the films

Copyright © 2013 VBRI press

shifted to lower wavelengths side with the increase of annealing temperature.

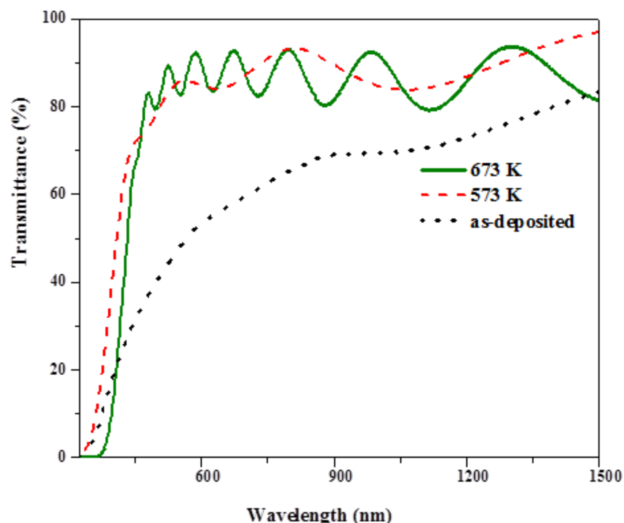

Fig. 5. Optical transmittance spectra of as-deposited and the MoO3 films annealed at different temperatures.

The optical absorption coefficient (α) of the films was evaluated from the optical transmittance (T) data using the relation,

$$\alpha = - (1/t) \ln T \qquad (4)$$

where t is the film thickness. The optical band gap of the films was calculated from the Tauc's **[33]** plots of $(\alpha h\upsilon)^2$ versus photon energy ($h\upsilon$) by assuming direct transition takes place in the films. The optical band gap of the as-deposited films was 2.98 eV. The band gap increased to 3.08 and 3.15 eV in the films annealed at 573 and 673 K respectively. As the annealing temperature increased the optical band gap of the film increased. Sivakumar et al**.** **[25]** achieved low optical band gap of 2.8 eV in the MoO_3 films formed at room temperature, while those deposited at 473 K showed lower band gap of 2.3 eV. In the literature, Navas et al. **[21]** reported that the optical band gap values of MoO_3 films were 3.77, 3.82 and 3.87 eV for as-deposited and the films annealed at 573 and 673 K respectively. Increase in band gap with annealing temperature can be attributed to the partial filling of oxygen vacancies. The band gap values are in consistent with the value of 3.16 and 3.27 eV obtained in electron beam evaporated films by Sain and reddy **[15]** for as-deposited and annealed MoO_3 films respectively.

The refractive index (n) of the films was determined from the optical transmittance interference data employing Swanepoel's envelope method employing the relation **[34],**

$$n(\lambda) = [N + (N^2 - n_0^2 n_1^2)^{1/2}]^{1/2} \qquad (5)$$

$$N = 2n_0 n_1[(T_M - T_m)/T_M T_m] + [(n_0^2 + n_1^2) / 2] \qquad (6)$$

where T_M and T_m are the optical transmittance maxima and minima and n_0 and n_1 the refractive indices of air and substrate respectively. The variation of refractive index with wavelength was shown in **Fig. 6**. The refractive index decreased with increase of annealing temperature. The refractive index (at wavelength of 600 nm) of the as-deposited film was 2.01 and increased to 2.08 with increase of annealing temperature to 673 K due to improvement in the crystallinity and packing density of the films. In contrast to this, Mohamed and Venkataraj **[27]** observed that the refractive index decreased with increase of annealing temperature up to 723 K, in the films formed at different sputter pressures, but after 773 K the refractive increased. Navas et al. **[35]** noticed that the refractive index of as-deposited films was 1.60 and decreased to 1.36 with the increase of annealing temperature to 673 K.

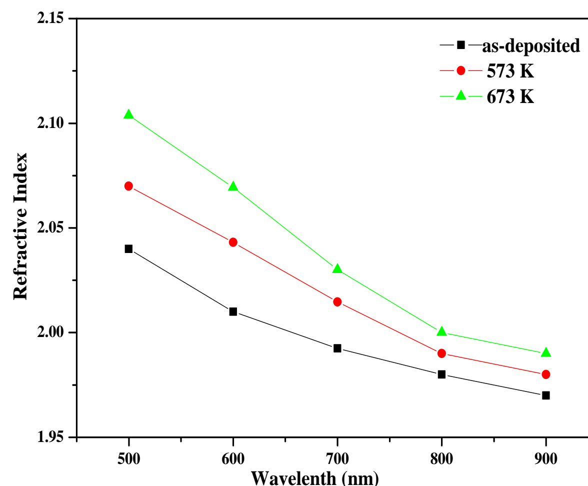

Fig. 6. Variation of refractive index with wavelength of as- deposited and annealed MoO_3 film.

Conclusion

Thin MoO_3 films were formed on Corning glass and silicon substrates held at room temperatures by sputtering of molybdenum target in an oxygen partial pressure of 4×10^{-4} mbar. The as-deposited films were annealed in air for two hours at temperatures in the range 573 - 673 K. X-ray diffraction studies revealed that the as-deposited films were amorphous in nature. Post-deposition annealing of films at 573 K was transformed into nanocrystalline with mixed phase of orthorhombic and monoclinic MoO_3. Further increase of annealing temperature to 673 K the crystallinity of the films improved. The crystallite size of the films increased from 32 to 39 nm with the increase of annealing temperature from 573 to 673 K respectively. The Fourier transform infrared transmittance spectra of the films indicated that the presence of characteristic vibrational modes of Mo = O and Mo – O – Mo related to the growth of MoO_3. Scanning electron micrographs of as-deposited films shows fine grain structure, nanoflower like structure growth in the films annealed at 573 K and nanodisk like structures at higher temperature of 673 K. The optical transmittance of the as-deposited films was about 60 % and it increased to 85 % with increase of annealing temperature to 673 K. The optical absorption edge of the films shifted towards lower wavelength side with increase of annealing temperatures. The optical band gap of the as-deposited films was 2.98 eV and it increased to 3.15 eV in the films annealed at 673 K. The refractive index of the as-deposited

Copyright © 2013 VBRI press

film was 2.01 and increased to 2.08 with increase of annealing temperature to 673 K due to improvement in the crystallinity and packing density of the films.

Reference

1. Mizushima, T.; Fukushima, K.; Ohkita, H.; Kakuta, H. *Appl. Catal A:* 2007, *326*, 106.
   DOI: 10.1016/j.apcata.2007.04.006.
2. Boudaoud, L.; Benramdana, N.; Desfeux, R.; Khalifa, B. Mathieu, C. *Catal. Today* 2006, *113*, 230.
   DOI: 10.1016/j.cattod.2005.11.072.
3. Chang, W.C.; Qi , X.; Kuo, J.C.; Lee, S.C.; Ng, S.K,; Chen, D. *Cryst. Eng. Commun*. 2011, *13*, 5125.
   DOI: 10.1039/C1CE05922J.
4. Lin, S.Y.; Wang, C.M.; Kao, K.S.; Chen, Y.C; Liu, C.C. *J. Sol-gel. Sci. Technol*. 2010, *53*, 51.
   DOI: 10.1007/s10971-009-2055-6.
5. Dhanasankar, M.; Purushothaman, K.K; Muralidharan, G. *Appl. Surf. Sci.* 2011, *257*, 2074.
   DOI: 10.1016/j.apsusc.2010.09.052.
6. Brezesnski, T.; Wang, J.; Tolbert, S.H.; Dunn, B. *Nat. Mater.* 2010, *9*, 146.
   DOI: 10.1038/nmat2612.
7. Yan, B.; Zheng, Z.; Zhang, J.; Gong, H., Shen, Z.; Huang, W.; Yu, T. *J. Phys. Chem. C,* 2009, *113*, 20259.
   DOI: 10.3139/146.110836.
8. Wu, M.C.; Lee, C.S. *Mater. Res. Bull*. 2009, *44*, 629.
   DOI: 10.1016/j.materresbull.2008.06.034.
9. Lin, S.Y.; Chen, Y.C., Wang, C.M.; Hseich, P.T.; Shih, *S.C. Appl. Surf. Sci.* 2009, *255,* 3868.
   DOI: 10.1016/j.apsusc.2008.10.069.
10. Prakash, A.; Tripathi, A.; Pivin, J.C.; Tripathi, J.; Chawla, A.K.; Ramesh Chandra.; Kim, S.S.; Ashokan, K.; Avasthi, D.K. *Adv. Mater. Lett.* 2011, *2 (1)*, 7.
    DOI: 10.5185/Amlett.2010.12187.
11. Intelligent Nanomaterials, *Wiley-Scrivener Pub. USA* (2012).
    ISBN: 978.0.470.93879.9.John Wiley and Sons.
12. Kocak, S.; Ertas, F.N.; Dursun, Z. Appl. Surf. Sci. 2013, *265,* 205.
    DOI: 10.1016/J.apsusc.2012.10.170.
13. Allogho, G.G.; Ashrit, P.V. *Thin Solid Films* 2012, *520,* 2326.
    DOI: 10.1016/J.tsf.2011.09.068.
14. Gretener, C.; Perrenoud, J.; Kranz, L.; Baechler, C.; Yoon, S.; Romanyuk, Y.E.; Buecheler, S.; Tiwari, A.N. *Thin Solid Films* 2012.
    DOI: 10.1016/j.tsf.2012.11.110.
15. Sain, T.S.; Reddy, G.B. *J. Appl. Phys.* 2005*, 98,* 026104.
    DOI: 10.1063/1.1949271.
16. Chen, J.S.; Cheah, Y.L.; Madhavi, S.; Lou, X.W. *J. Phys. Chem. C* 2010, *114*, 8675.
    DOI:10.1021/jp1102109
17. Ramana, C.V.; Julien, C.M. *Chem. Phys. Lett. 2006, 428,* 114.
    DOI: 10.1016/j.cplett.2006.06.117.
18. Nirupama, V.; Gunasekhar, K.R.; Sreedhar, B.; Uthanna, S. *Curr. Appl. Phys*. 2010, *10*, 272.
    DOI: 10.1016/j.cap.2009.06.005.
19. Uthanna, S.; Nirupama, V.; Pierson, J.F. *Appl. Surf. Sci*. 2010, *256*, 3133.
    DOI: 10.1016/j.apsusc.2009.11.086.
20. Srinivasa Rao, K; Rajini Kanth, B.; Mukhopadhyay, P.K. *Appl. Phys. A* 2009, *9*, 985.
    DOI: 10.1007/S00339.009.5132.3.
21. Navas, I.; Vinod Kumar, R.; Lethy, K.J.; Detty, A.P.; Ganesan, V.; Sathe, V.; Mahadevan Pillai, V.P. *J. Phys. D: Appl. Phys*. 2009, *42*, 175305.
    DOI: 10.1088/0022-3727/42/17/175305.
22. Diskus, M.; Nilson, O.; Fjellveg, H. J. *Mater. Chem*. 2011, *21*, 705.
    DOI: 10.1039/C0JM01099E.
23. Patil, R.S.; Uplane, M.D.; Patil, P.S. *Appl. Surf. Sci.* 2006, *252*, 8050.
    DOI: 10.1016/j.apsusc.2005.10.016.
24. Martinez, H.M.; Torres, J.; Lopez Correno, L.D.; Rodriguez-Garcia, M.E. *Mater. Character.* 2013, *25*, 184.
    DOI: 10.1016/j.matchar.2012.11.002.
25. Sivakumar, R.; Gopalakrishnan, R.; Jayachandran, M.; Sanjeeviraja, C. *Curr. Appl. Phys.* 2007, *7*, 51.
    DOI: 10.1016/j.cap.2005.10.001.
26. Hsu, C.S.; Chan, C.C.; Huang, C.T.; Peng, C.H.; Hsu, W.C. *Thin Solid Films* 2008, *516*, 4839.
    DOI: 10.1016/j.tsf.2007.09.019.
27. Mohamed, S.H.; Venkatraj, S. *Vacuum* 2007, *81*, 636.
    DOI: 10.1016/j.vacuum.2006.08.006.
28. Fan, X.; Fang, G.; Qin, P.; Sun, N.; Liu, N.; Zheng, Q.; Cheng, F.; Yuan, L.; Zhao, X. *J. Phys. D: Appl. Phys*. 2011, *44*, 045101.
    DOI: 10.1088/0022-3727/44/4/045101.
29. Yang, W.Q.; Wei, Z.R.; Zhu, X.H.; Yang, D.Y.; *Phys. Lett. A,* 2009, *373*, 3965.
    DOI: 10.1016/j. Physleta 2009.08.058.
30. Cullity, B.D. Elements of X-ray Diffraction, *IInd Ed, Addison Wesley, London*. 1978.
    DOI: 10.1107/S0567739479000917.
31. Lalitha, S.; Sathyamurthy, R.; Senthilarasu, S.; Subbarayan, A.; Natarajan, K. *Solar Energy Mater. Solar Cells*. 2004, *82*, 187.
    DOI: 10.1016/j.solmat.2004.01.017.
32. Ivanova, T.; Gesheva, K.A.; Szekeres, A. *J. Solid State Electrochem*. 2002, *7*, 21.
    DOI: 10.1007/s 10008 002-0274-7.
33. Tauc,J." Amorphous and Liquid Semiconductors", Plenum Press, New York 1974.
34. Swanepoel, R.J. *J. Phys. E: Sci. Instrum*. 1983, *16*, 1214.
    DOI: 10.1007/s00339-010-5632-1.
35. Navas, I; Vinod Kumar R ; Detty, A.P; Mahadevan Pillai, V.P. *Mater. Sci. Eng.* 2009, *2*, 012035.
    DOI: 10.1088/1757-899X/2/1/012035.

Advanced Materials Letters

Publish your article in this journal

ADVANCED MATERIALS Letters is an international journal published quarterly. The journal is intended to provide top-quality peer-reviewed research papers in the fascinating field of materials science particularly in the area of structure, synthesis and processing, characterization, advanced-state properties, and applications of materials. All articles are indexed on various databases including DOAJ and are available for download for free. The manuscript management system is completely electronic and has fast and fair peer-review process. The journal includes review articles, research articles, notes, letter to editor and short communications.

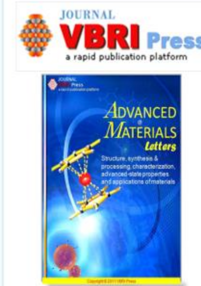

Copyright © 2013 VBRI press